Plasmon resonances and tachyon ghost modes in highly conducting sheets

D. O. Oriekhov[1] and L. S. Levitov[2]
[1]*Department of Physics, Taras Shevchenko National University of Kiev, Kiev 03680, Ukraine*
[2]*Massachusetts Institute of Technology, Cambridge, Massachusetts 02139, USA*

(Received 26 March 2019; revised manuscript received 19 May 2020; accepted 20 May 2020; published 12 June 2020)

Plasmon-polariton modes in two-dimensional electron gases have a dual field-matter nature that endows them with unusual properties when electrical conductivity exceeds a certain threshold set by the speed of light. In this regime plasmons display an interesting relation with tachyons, the hypothetical faster-than-light particles. While not directly observable, tachyons directly impact properties of plasmon modes. Namely, in the "tachyon" regime, plasmon resonances remain sharp even when the carrier collision rate γ exceeds plasmon resonance frequency. Resonances feature a recurrent behavior as γ increases, first broadening and then narrowing and acquiring asymmetric non-Lorentzian line shapes with power-law tails extending into the tachyon continuum $\omega > ck$. This unusual behavior can be linked to the properties of tachyon poles located beneath $\omega > ck$ branch cuts in the complex ω plane: as γ grows, tachyon poles approach the light cone and hybridize with plasmons. Narrow resonances persisting for $\gamma > \omega$, along with the unusual density and temperature dependence of resonance frequencies, provide clear signatures of the tachyon regime.

DOI: 10.1103/PhysRevB.101.245136

I. INTRODUCTION

Surface plasmon-polaritons in atomically thin electron systems feature a number of interesting and potentially useful properties, such as strong light-matter interaction and field confinement, as well as gate tunability [1–6]. Plasmon modes, owing to their hybrid charge-field character, enable a powerful near-field diagnostic for electronic properties of two-dimensional (2D) materials [7,8]. The synchronized movement of charges in different spatial regions, which constitutes plasma oscillations, is sustained by long-range electron-electron interactions. In that, the effects of EM retardation due to the finite speed of light are typically small, since electron velocities in solids are nonrelativistic [9]. Nonetheless, since models based on nonretarded Coulomb interactions predict $\omega \sim \sqrt{k}$ dispersion with group velocity diverging at small k, the relativistic retardation effects inevitably become prominent in the long-wavelength limit. Strong retardation endows the plasmon-polariton modes with interesting dynamical memory effects inherent to the 3D/2D field-matter binding in the long-wavelength regime [10–12].

Can retardation-dominated modes be accessed without changing the plasmon wavelength? This question was first posed by Falko and Khmelnitskii [13], who predicted enhancement of retardation effects upon increasing the conductivity of the electron gas. Reference [13] also uncovered a truly puzzling behavior—collective modes resembling tachyons, the hypothetical superluminal particles. The regime of interest is reached when the dc ohmic conductivity exceeds the threshold set by the speed of light:

$$\sigma > \sqrt{\varepsilon}c/2\pi \quad (\text{in SI units: } \sigma > 2\sqrt{\varepsilon\varepsilon_0/\mu_0}), \qquad (1)$$

where the factor $\sqrt{\varepsilon}$ accounts for the dielectric environment (below we use $\sqrt{\varepsilon} = 1$ unless stated otherwise). In cgs units, used in Eq. (1), ohmic conductivity has dimension of velocity, wherein $2\pi/c \approx 188\,\Omega$ per square [14]. Such values are routinely reachable in state-of-the-art 2D electron systems [10–12]. Reference [13], by analyzing the dynamics of 2D currents coupled to 3D electromagnetic fields, obtained modes which, if taken for granted, would describe excitations traveling at superluminal speeds. This would of course violate the known laws of physics, leading to a conclusion that these are some kind of ghost modes that cannot be observed directly. Despite several attempts to clarify the meaning of these findings [11,12,15], their relation to observable quantities has remained uncertain.

II. PLASMON RESONANCES AT HIGH COLLISION RATES $\gamma \gg \omega$

With this motivation in mind, here we analyze plasmon resonances and their relation to tachyon modes. We focus on the charge-potential linear response function of a 2D conducting sheet, $\rho_{\omega,k} = -D(\omega,k)\phi_{\omega,k}$. The dynamical compressibility $D(\omega,k)$ is found to be expressed through the dispersive sheet conductivity $\sigma(\omega)$ as

$$D(\omega,k) = \frac{k^2\sigma(\omega)}{2\pi q(\omega)\sigma(\omega) - i\omega}, \quad q(\omega) = \sqrt{k^2 - \frac{\omega^2}{c^2}}. \qquad (2)$$

The conductivity, in general, depends also on the wave number k and the *ee* scattering rates. However, these effects are important only at relatively large values $k \sim \omega/v_F$, whereas the values relevant in our case are much smaller: $k \sim \omega/c$. The dielectric constant of the surrounding medium, ignored here for simplicity, will be accounted for below; see Eq. (18).

The spectral function $\mathrm{Im}\,D(\omega,k)$ describes plasmon resonances in several different regimes. At $\sigma > c/2\pi$, the resonances acquire an interesting recurrent character, which is illustrated in Fig. 1. As the collision rate γ grows, with

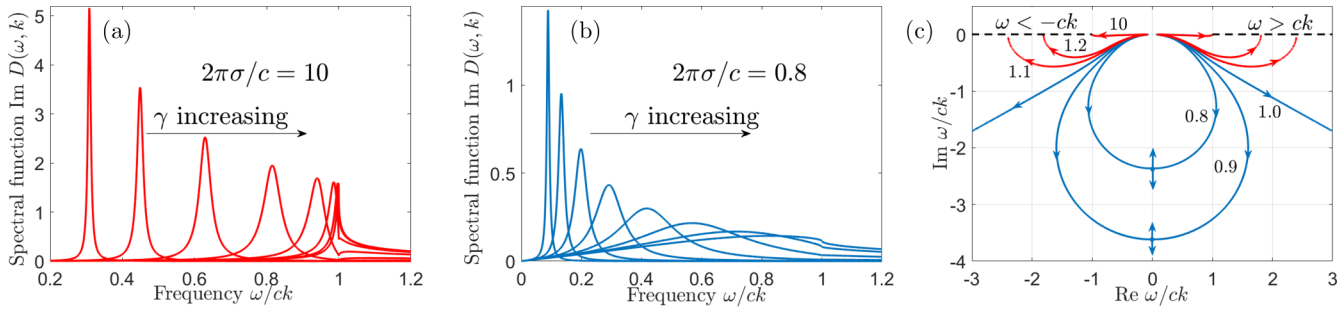

FIG. 1. (a) Recurrent behavior of plasmon resonances in the "tachyon" regime $\sigma > c/2\pi$. Plotted is the dynamic compressibility Im $D(\omega, k)$, Eq. (2), at a fixed σ. Resonances evolve nonmonotonically as the collision rate γ grows, first broadening, then sharpening and developing non-Lorentzian line shapes, while the resonance frequency becomes pinned at $\omega \approx ck$ value. (b) Nonrecurrent behavior at $\sigma < c/2\pi$: resonances broaden and become overdamped as γ increases. (c) Pole trajectories, obtained from Eq. (4) at a fixed σ. Arrows show the direction of pole movement at increasing γ; numbers indicate $2\pi\sigma/c$ values. For $2\pi\sigma > c$, the poles move under the branch cuts of the square roots in Eq. (2) (dashed lines). Positioned under branch cuts, the poles represent the Falko-Khmelnitskii tachyons, Eq. (7). The latter, despite being undamped, Im $\omega = 0$, do not generate propagating modes.

the conductivity σ and wave number k values kept fixed, resonances first broaden, but then, when γ exceeds ck, they begin to sharpen as γ increases. Simultaneously, resonance frequency becomes pinned at $\omega = ck$ value and line shapes change from Lorentzian to highly non-Lorentzian. Strikingly, resonances remain sharp even when the collision rate γ is much greater than the resonance frequency ω. In this regime, line shapes become asymmetrical, cuspy, and develop tails extending far into the $\omega > ck$ continuum. At $\sigma < c/2\pi$, on the contrary, a conventional behavior takes place: resonances broaden and weaken as γ grows.

The physical reason for resonances sharpening can be understood as a reduction in damping due to a change in the mode makeup upon frequency approaching ck. Indeed, at $\omega < ck$ the field outside the conducting sheet represents an evanescent wave decaying as a function of distance as $e^{-\lambda z}$ with the decay parameter $\lambda = q(\omega)$. Since the latter becomes small as ω approaches ck, the mode confinement in the direction perpendicular to the plane becomes less tight, leading to an enhancement in the field-matter volume ratio. This makes the mode overlap with two-dimensional electrons smaller and, therefore, reduces damping. Here and below we assume that dissipation is dominated by ohmic losses of 2D electrons; the situation in experimental systems can be more complicated due to losses in the surrounding medium.

Plasmon resonances that sharpen when the collision rate γ exceeds resonance frequency also suggest an interpretation in terms of motional narrowing. A resonant frequency that has a smaller linewidth than may be expected is a common behavior in systems where oscillations occur in the presence of a rapidly changing environment. The motional narrowing effect arises due to the changes quickly averaging out in accordance with the central limit theorem, and therefore decoupling from the oscillating degrees of freedom. For plasmon resonances, motional narrowing is often regarded as a signature of the hydrodynamic regime in which plasmon excitation is shared among many particles that quickly exchange their microscopic states through two-body scattering. In contrast, the present problem presents an unusual situation when motional narrowing results from oscillations that are supported by a large number of quickly relaxing degrees of freedom, producing resonances that remain sharp even at high collision rates $\gamma \gg \omega$.

In experiment, the key system parameters—γ and σ—can be varied independently by tuning temperature and carrier density (T and n). However, since in general the T and n dependence of γ and σ may be fairly complicated, here it will be convenient to view these quantities as proxies for the experimental knobs, treating them as independently tunable variables. This represents a meaningful choice also because the quantity σ is directly measurable, and thus the recurrent evolution of resonances at a fixed σ and varying γ, such as that shown in Figs. 1 and 2, can be extracted directly from the measurement results without knowing the exact dependence of γ and σ on the experimental knobs such as T and n.

Quantitative estimates suggest that the regime of interest is readily accessible in atomically thin materials currently under investigation in nanoscale plasmonics [1–8]. Namely, in graphene, the carrier mean free path can be as large as 10–20 μm, exceeding by a large margin the values $\sim$1 μm set by the threshold in Eq. (1). These aspects are discussed in greater detail in Secs. IV and V.

It is also interesting to mention that superluminal modes somewhat reminiscent of our tachyons have appeared previously in the literature on the surface Zenneck wave problem. The Zenneck wave propagates at the surface of a lossy medium in a three-dimensional space (see Refs. [16–18] and references therein); Maxwell equations describing these waves admit solutions with superluminal dispersion $\omega = c'k$, $c' > c$. However, the puzzling superluminal aspects aside, our ghost modes are distinct from those in the Zenneck problem. One difference is dimensionality (2D vs 3D); another is the character of the EM field—residing within the lossy medium vs the free space outside the conducting sheet, respectively. Even more important is the different character of the observable. The Zenneck wave can manifest itself through resonances with radiation incident from 3D at a certain angle [16,19]. In contrast, our tachyon modes manifest themselves through resonances in the dynamical response functions. The relation between our problem and the Zenneck wave problem will be discussed in more detail elsewhere.

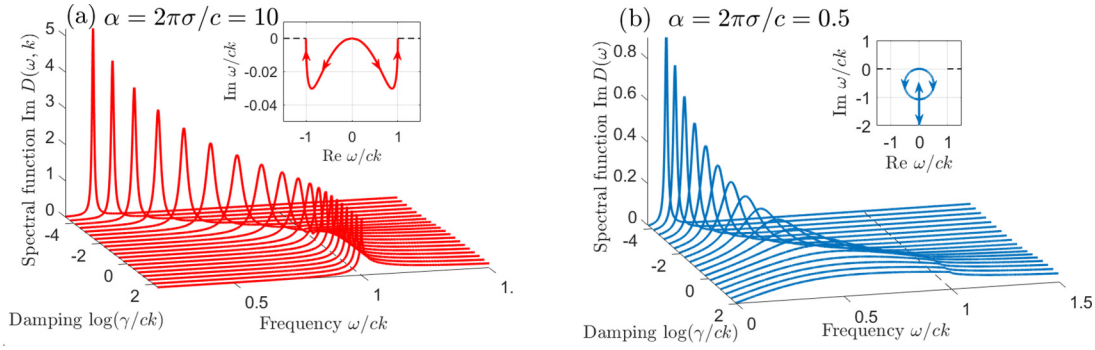

FIG. 2. Frame-by-frame evolution of the resonances in Fig. 1. (a) At a constant $\sigma > c/2\pi$, resonances are dispersing as the collision rate grows from $\gamma \ll ck$ to $\gamma \sim ck$; the dispersion is quenched for $\gamma > ck$. In the latter case the nondispersing resonance frequency becomes pinned at the edge of the continuum $\omega > ck$, taking values $\omega \approx ck$. The dependence of the resonance width vs γ is nonmonotonic, broadening while $\gamma < ck$ and narrowing once γ exceeds ck. (b) Conventional behavior at $\sigma < c/2\pi$: resonances broaden as γ grows and are washed out once γ exceeds the resonance frequency. Insets in (a) and (b) show the trajectories of $D(\omega, k)$ poles in the complex ω plane, obtained by varying γ.

III. RESONANCE SHARPENING DUE TO TACHYON POLES NEAR THE LIGHT CONE

A unique insight into the properties of the resonances, in particular, their relation with the tachyon modes of Ref. [13], can be gained by investigating complex-ω poles of $D(\omega, k)$. Here we focus on the dispersive Drude model:

$$i\omega = 2\pi q(\omega)\sigma(\omega), \quad \sigma(\omega) = \frac{ne^2}{m(\gamma - i\omega)}. \tag{3}$$

The dispersion relation (3), after simple algebra, yields a characteristic equation

$$\frac{\omega^2(\omega + i\gamma)^2}{\beta^2} + \frac{\omega^2}{c^2} = k^2, \quad \beta = \frac{2\pi ne^2}{m}. \tag{4}$$

The complex roots of this quartic equation can be found explicitly. Two of these roots are the poles of $D(\omega, k)$ shown in Fig. 1(c). Two spurious roots, added when the square root in $q(\omega)$ is rationalized, are discarded.

The behavior of poles in the complex ω plane, which is illustrated in Fig. 1(c), mimics the recurrent behavior of resonances in the "tachyon" regime $\sigma > c/2\pi$: as γ increases and σ is kept fixed, the poles first move away from the real ω axis, then make a U-turn and move back towards the real axis, landing on the lower side of the branch cuts $\omega < -ck$ and $\omega > ck$. Likewise, at $\sigma < c/2\pi$ pole trajectories show a nonrecurrent behavior: moving gradually away from the real axis without turning back, and then colliding at the imaginary axis to create a pair of overdamped modes with pure imaginary ω.

Quantitatively, this behavior can be described most easily by taking the limit $2\pi\sigma \gg c$ in Eq. (4). In this case, as Fig. 1 suggests, the real part of ω is much greater than the imaginary part. Ignoring the latter at first, we take the $\omega \gg \gamma$ limit. This yields a dependence

$$k^2 = \frac{\omega^4}{\beta^2} + \frac{\omega^2}{c^2}, \tag{5}$$

which gives the dispersion $\omega = (\beta k)^{1/2}$ at large k, and a light-like dispersion $\omega = ck$ at small k, as expected. The imaginary part of ω, which provides an estimate for resonance width, can be found by replacing $\omega \to \omega - i\Gamma$, and expanding in small γ and Γ to first order. This gives

$$\Gamma = \frac{\omega^2\gamma}{2\omega^2 + \frac{\beta^2}{c^2}}. \tag{6}$$

Substituting $\beta = 2\pi\sigma\gamma$ and taking σ to be constant, we see that Eq. (6) predicts a nonmonotonic dependence for Γ vs γ. For the resonance width, estimated as Γ, this behavior is in good agreement with the recurrent evolution of resonances and poles at varying γ and constant σ, as shown in Fig. 1 and, in greater detail, in Fig. 2.

At $2\pi\sigma \gtrsim c$ and high damping γ, the poles of $D(\omega, k)$ are positioned directly beneath the branch cuts (see Fig. 3). In the limit $\gamma \gg \omega$, after approximating $\sigma(\omega) \approx \sigma + \frac{i\omega}{\gamma}\sigma$, simple algebra gives

$$\omega_\pm = \pm vk - i\gamma', \quad v = \frac{c\alpha}{\sqrt{\alpha^2 - 1}}, \quad \alpha = \frac{2\pi\sigma}{c}, \tag{7}$$

which are the values identical to those found in Ref. [13], with damping $\gamma' = \frac{\alpha^2c^2k^2}{\gamma(\alpha^2-1)^2}$ vanishing at high γ. As noted in Ref. [13], the peculiar dispersion relation with greater-than-c group velocity does not imply superluminal signal propagation. The reasons for that, which are somewhat subtle, can be summarized as follows.

First, since at large γ the frequencies $\omega_\pm$ reside directly at the branch cuts $\omega > ck$ and $\omega < -ck$, the poles $\omega = \omega_\pm$ do not represent isolated singularities; rather the poles and branch cuts must be handled jointly as *compound*, or *unseparable,* singularities. Another point of note, which is more essential than the "compound singularity" property, is that the poles reside on the lower (unphysical) sides of the branch cuts, which separate the poles from the upper imaginary half plane $\mathrm{Im}\,\omega > 0$. Since it is the ω dependence in that half plane that governs time evolution of a response, the poles separated from the $\mathrm{Im}\,\omega > 0$ domain by branch cuts cannot create, on their own, any $v > c$ modes. More formally, below we demonstrate that these poles give no singular contributions to the spectral function because their residues vanish; see Eq. (12) and accompanying discussion. Instead, the poles under the branch cuts alter the shapes of the resonances positioned at $\omega \lesssim ck$, which remain sharp even when $\gamma \gg \omega$

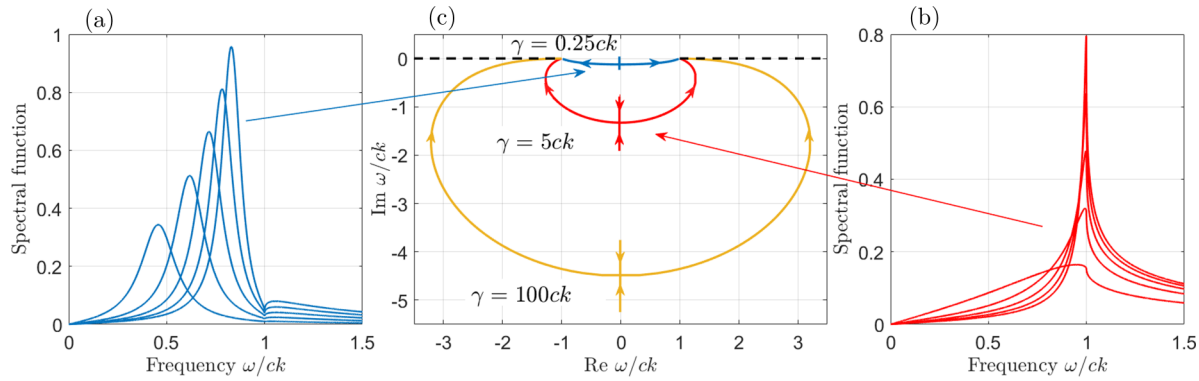

FIG. 3. (a),(b) Evolution of resonances at a fixed γ upon $2\pi\sigma/c$ increasing from 1 to 5. Resonances sharpen as σ increases; in (b) they sharpen and narrow down despite the fact that the resonance frequency remains smaller than γ. (c) Pole trajectories found from Eq. (4) plotted at a fixed γ for $2\pi\sigma/c$ varying from 0.01 to 20. The direction of pole movement is indicated by arrows. The light-cone branch cuts $|\omega| > c|k|$ are shown by dashed lines; γ values are indicated next to arrows. Tachyon modes arise at large σ as the poles move towards the branch cuts; the resonances sharpen as the tachyon poles approach the light cone $\omega = ck$.

but acquire asymmetric line shapes with the tails extending into the tachyon continuum $\omega > ck$.

IV. EXPERIMENTAL ACCESSIBILITY OF THE "SUPERLUMINAL" REGIME $\sigma > c/2\pi$

Here we provide quantitative estimates which illustrate that the regime $\sigma > c/2\pi$ is readily accessible in atomically thin conductors such as graphene monolayer and bilayer. To facilitate estimates, we write Drude conductivity as

$$\sigma = \frac{ne^2}{m}\tau = \frac{g_v g_s}{4\pi}\frac{e^2}{\hbar}k_F\ell,$$

where k_F and ℓ are the electron Fermi momentum and mean free path values and $g_s = g_v = 2$ describes the spin and valley degeneracy. Using this result, the relation $\sigma > c/2\pi$ can be written as a condition for the mean free path:

$$\ell > \frac{\hbar c}{e^2}\frac{1}{2k_F}. \tag{8}$$

Evaluating k_F for a typical carrier concentration $n = 10^{12}$ cm^{-2} we obtain the value $\frac{1}{2k_F} \approx 9$ nm. Multiplying this result by $\frac{\hbar c}{e^2} \approx 137$ brings the condition in Eq. (8) to the form

$$\ell > 1.2\ \mu\text{m}.$$

However, the mean free path values in high-mobility graphene monolayer and bilayer routinely reach 10–20 μm, which is comfortably in the range set by the bound in Eq. (8). This indicates that the condition $\sigma > c/2\pi$ can be easily met.

The condition $\sigma > c/2\pi$ can also be achieved in metallic few-atom-thin films, a system where surface plasmons have been investigated recently [20]. In thin films, the carrier mean free path is limited by the film thickness, i.e., is relatively short. However, the carrier density in films is much greater than in graphene. For example, for a few-nanometer-thin film the effective 2D carrier density is on the order $n \approx 10^{17}$ cm^{-2}, whereas $\ell \approx 1$ nm. Comparing to the above we see that the shorter mean free path value is balanced by the larger k_F value, so that the condition $\sigma > c/2\pi$ remains reachable.

V. THE "SUPERLUMINAL" PLASMONIC RESPONSE

To validate the picture discussed in Secs. I and II, we consider the charge-potential response in the time domain:

$$\rho_k(t) = -\int_{-\infty}^{\infty} dt' D_k(t-t')\phi_k(t'), \tag{9}$$

corresponding to $\rho_{\omega,k} = -D(\omega,k)\phi_{\omega,k}$ at a fixed wave number k. The memory function $D_k(t-t')$ equals

$$D_k(\tau) = \int_{-\infty}^{\infty}\frac{d\omega}{2\pi}e^{-i\omega\tau}D(\omega,k). \tag{10}$$

Here the integral runs over a straight path $-\infty < \omega < \infty$ just above the real axis. The causality condition $D_k(\tau < 0) = 0$ is ensured, as always, by analyticity of $D(\omega,k)$ in the upper half plane $\text{Im}\,\omega > 0$.

To see why the expression in Eq. (2), when plugged into Eq. (10), does not generate propagating modes with $v > c$, we start with a simple technical observation regarding analytic properties of $q(\omega)$. The quantity $q(\omega)$ is real in the domain $-ck < \omega < ck$ and purely imaginary at $\omega > ck$ and $\omega < -ck$ with a sign that must be determined by analytic continuation. The recipe for continuation follows from analyticity of $q(\omega)$ in the half plane $\text{Im}\,\omega > 0$, prescribed by causality. Therefore, $q(\omega)$ should be treated as $\sqrt{k^2 - \frac{(\omega+i0)^2}{c^2}}$ with an infinitesimal positive shift in ω, giving

$$q(\omega) = \begin{cases} \sqrt{k^2 - \frac{\omega^2}{c^2}}, & -ck < \omega < ck, \\ -i\,\text{sgn}\,\omega\sqrt{\frac{\omega^2}{c^2} - k^2}, & \omega < -ck,\ \omega > ck, \end{cases} \tag{11}$$

where the sign factor $-\text{sgn}\,\omega$ for the cases $\omega > ck$ and $\omega < -ck$ arises due to analytic continuation through the upper half plane. A simple consequence of this result is that the dispersion equation obtained in Ref. [13] does not have solutions at the real axis on the upper side of branch cuts. The solutions given in (7) are located under the cuts $\omega > ck$ and $\omega < -ck$. Therefore, from the point of view of analytical properties, they represent fictitious poles or, more precisely, the poles located on a nonphysical sheet of the Riemann

surface of complex frequency ω. As such, they do not generate propagating modes.

This point can be illustrated by transforming the expression in Eq. (2) in the $\gamma \gg \omega$ limit to the form

$$D(\omega, k) = \frac{\alpha c k^2 (\alpha \sqrt{c^2 k^2 - \omega^2} + i\omega)}{\alpha^2 c^2 k^2 - (\alpha^2 - 1)\omega^2}, \tag{12}$$

where we replaced $\sigma(\omega)$ in Eq. (2) by $\sigma = c\alpha/2\pi$, and rationalized the denominator by multiplying it by $\alpha\sqrt{c^2k^2 - \omega^2} + i\omega$. This expression has poles on the real axis at the tachyon frequencies $\omega = \pm vk$ with $v > c$, Eq. (7), so long as $\alpha > 1$. However, these poles give a vanishing contribution to the spectral function evaluated at $\mathrm{Im}\,\omega = +i0$ because the numerator, owing to the sign prescription found above, Eq. (11), vanishes at the poles. As a result, the spectral function is smooth at the tachyon frequencies $|\omega| > ck$. This is clearly seen in the resonances shown in Figs. 1 and 2, which have smooth tails extending into the tachyon continuum with cusps at $\omega = ck$ but no singularities at $\omega > ck$.

Next, we proceed to derive the response function given in Eq. (2) and estimate the relevant experimental parameter values. We start with EM equations in 3D space due to 2D currents, for generality adding a dielectric constant of the surrounding medium. Using Fourier harmonics, in Lorentz gauge we have $\boldsymbol{k}\cdot\boldsymbol{A}_{\boldsymbol{k},\omega} - \frac{\omega}{c}\varepsilon\phi_{\boldsymbol{k},\omega} = 0$, and

$$\Big(k^2 - \frac{\omega^2}{c^2}\varepsilon\Big)\boldsymbol{A}_{\boldsymbol{k},\omega} = \frac{4\pi}{c}\boldsymbol{j}_{\boldsymbol{k},\omega}, \quad \Big(k^2 - \frac{\omega^2}{c^2}\varepsilon\Big)\phi_{\boldsymbol{k},\omega} = \frac{4\pi}{\varepsilon}\rho_{\boldsymbol{k},\omega}.$$

Taking z axis to be perpendicular to the 2D sheet, and working in a mixed Fourier representation,

$$\phi_{\boldsymbol{k},\omega}(z) = \sum_{k_z} \phi_{\boldsymbol{k},\omega} e^{ik_z z}, \quad \rho_{\boldsymbol{k},\omega}(z) = \sum_{k_z} \rho_{\boldsymbol{k},\omega} e^{ik_z z},$$

where from now on $\boldsymbol{k}$ is two dimensional, we have

$$\Big(\partial_z^2 - k^2 + \frac{\omega^2}{c^2}\varepsilon\Big)\phi_{\boldsymbol{k},\omega}(z) = -\frac{4\pi}{\varepsilon}\rho_{\boldsymbol{k},\omega}\delta(z), \tag{13}$$

$$\Big(\partial_z^2 - k^2 + \frac{\omega^2}{c^2}\varepsilon\Big)\boldsymbol{A}_{\boldsymbol{k},\omega}(z) = -\frac{4\pi}{c}\boldsymbol{j}_{\boldsymbol{k},\omega}\delta(z). \tag{14}$$

Solving Eqs. (13) and (14) for the z dependence gives

$$\phi_{\boldsymbol{k},\omega}(z) = \frac{2\pi\rho_{\boldsymbol{k},\omega}}{\varepsilon q(\omega)} e^{-q(\omega)|z|}, \quad \boldsymbol{A}_{\boldsymbol{k},\omega}(z) = \frac{2\pi\boldsymbol{j}_{\boldsymbol{k},\omega}}{cq(\omega)} e^{-q(\omega)|z|}, \tag{15}$$

with $q(\omega) = \sqrt{k^2 - \frac{\omega^2}{c^2}\varepsilon}$.

These relations must be combined with the conductivity response $\boldsymbol{j}' = \sigma(\omega)\boldsymbol{E}$. Here the prime indicates the induced current, whereas the quantities in Eq. (15) should be taken as sums of the external and induced contributions, $\rho = \rho' + \rho_{\mathrm{ext}}$ and $\boldsymbol{j} = \boldsymbol{j}' + \boldsymbol{j}_{\mathrm{ext}}$. Writing $\boldsymbol{E} = -\nabla\phi - \frac{1}{c}\partial_t\boldsymbol{A}$ and using the continuity relations for the 2D currents and charges, $\rho_{k,\omega} = \frac{1}{\omega}\boldsymbol{k}\cdot\boldsymbol{j}_{k,\omega}$, we eliminate variables ρ and ϕ to obtain

$$\boldsymbol{j}'_{\boldsymbol{k},\omega} = i\omega\frac{2\pi\sigma(\omega)}{q(\omega)c^2}\left(\boldsymbol{j}_{\boldsymbol{k},\omega} - \frac{c^2}{\omega^2\varepsilon}\boldsymbol{k}(\boldsymbol{k}\cdot\boldsymbol{j}_{\boldsymbol{k},\omega})\right), \tag{16}$$

with $\boldsymbol{j} = \boldsymbol{j}' + \boldsymbol{j}_{\mathrm{ext}}$. This relation can be put in the form of a 2×2 matrix response function, $\boldsymbol{j}'_{\boldsymbol{k},\omega} = M(\boldsymbol{j}'_{\boldsymbol{k},\omega} + \boldsymbol{j}^{\mathrm{ext}}_{\boldsymbol{k},\omega})$. For longitudinal waves $\boldsymbol{j}_{\boldsymbol{k},\omega} \parallel \boldsymbol{k}$, $\boldsymbol{j}^{\mathrm{ext}}_{\boldsymbol{k},\omega} \parallel \boldsymbol{k}$ we obtain

$$\boldsymbol{j}_{\boldsymbol{k},\omega} = \frac{1}{1-M}\boldsymbol{j}^{\mathrm{ext}}_{\boldsymbol{k},\omega} = \frac{i\omega\varepsilon}{i\omega\varepsilon - 2\pi q(\omega)\sigma(\omega)}\boldsymbol{j}^{\mathrm{ext}}_{\boldsymbol{k},\omega}. \tag{17}$$

Dynamical compressibility can now be found by substituting in place of $\boldsymbol{j}^{\mathrm{ext}}_{\boldsymbol{k},\omega}$ the current induced by an external potential, $-i\sigma(\omega)\boldsymbol{k}\phi^{\mathrm{ext}}_{\boldsymbol{k},\omega}$. Relating the net current $\boldsymbol{j} = \boldsymbol{j}' + \boldsymbol{j}_{\mathrm{ext}}$ to the net charge as $\rho = \frac{1}{\omega}\boldsymbol{k}\cdot\boldsymbol{j}$ gives

$$\rho_{\omega,k} = \frac{k^2\sigma(\omega)\varepsilon}{i\omega\varepsilon - 2\pi q(\omega)\sigma(\omega)}\phi^{\mathrm{ext}}_{\omega,k}, \tag{18}$$

which is the result in Eq. (2) generalized to $\varepsilon \neq 1$. As a sanity check, at $\omega = 0$ we recover the standard result for an ideal conductor $\rho_k = -\frac{\varepsilon k}{2\pi}\phi_k$, where the minus sign describes perfect screening of an external potential by induced charges.

The result in Eq. (18) can be related to the $\varepsilon = 1$ result in Eq. (2) by absorbing ε into rescaled parameters,

$$c \to \tilde{c} = \frac{c}{\sqrt{\varepsilon}}, \quad \sigma \to \tilde{\sigma} = \frac{\sigma}{\varepsilon}, \tag{19}$$

upon which the dimensionless ratio $\alpha = 2\pi\sigma/c$ is reduced by a factor $\sqrt{\varepsilon}$. Accounting for this change, the results above can be applied directly, with the condition in Eq. (1) replaced by $\sigma > \frac{\sqrt{\varepsilon}c}{2\pi}$, and so on. For a system of size $L = 20\ \mu$m, using the value $\varepsilon \approx 11$ (sapphire), the resonance frequency is $\omega_0 = \frac{\pi c}{\sqrt{\varepsilon}L} = 2\pi \times 2.26$ THz. This value can be reduced by using proximal gates to screen the electron-electron interactions.

VI. DISCUSSION AND CONCLUSIONS

Plasmon resonance sharpening, occurring when the collision rate exceeds the resonance frequency, $\gamma \gg \omega$, is a striking behavior that can be attributed to motional narrowing due to many quickly relaxing microscopic degrees of freedom that plasmon excitations are made of. Motional narrowing of collective modes is of course familiar in the hydrodynamic regime, taking place in plasmonics when plasmon frequency is smaller than the electron-electron scattering rate, $\omega \ll \gamma_{\mathrm{ee}}$. Here we encounter a more exotic behavior: resonance sharpening through motional narrowing arising due to rapid momentum-relaxing collisions. It is usually taken for granted that high collision rates $\gamma \gg \omega$ produce rapid damping that broadens plasmon resonances. However, as the discussion above demonstrates, this simple intuition fails for electron systems with conductivity taking high "superluminal" values $\sigma > c/2\pi$. In this case, perhaps somewhat counterintuitively, rapid relaxation gives rise to abnormally narrow resonances.

This surprising behavior can also be linked to the peculiar evolution of poles of the response function in the complex frequency plane. At small γ the poles represent the conventional collisionless plasmons. As γ grows, the poles move under the branch cuts, turning into tachyon modes with faster-than-c group velocity, first predicted by Falko and Khmelnitskii. Since the poles are positioned on the unphysical sheet of the complex frequency Riemann surface, they do not result, by themselves, in propagating modes. However, as these superluminal poles approach the light cone $\omega = ck$, they influence the observable response by producing plasmon resonances

with distinct non-Lorentzian line shapes and sharpening them despite the collision rate being high. These features, along with a characteristic nonmonotonic dependence on experimental knobs, provide clear signatures of the tachyon regime. The relation between tachyon poles and plasmonic resonances that sharpen when conductivity increases above the threshold value set by the speed of light can therefore be useful as a way to probe the elusive tachyon modes.

ACKNOWLEDGMENTS

We are grateful to I. V. Kukushkin and K. E. Nagaev for useful discussions. L.L. acknowledges support from the Science and Technology Center for Integrated Quantum Materials, NSF Grant No. DMR-1231319. Part of this work was performed at the Aspen Center for Physics, which is supported by National Science Foundation Grant No. PHY-1607611.

[1] B. Wunsch, T. Stauber, F. Sols, and F. Guinea, Dynamical polarization of graphene at finite doping, New J. Phys. **8**, 318 (2006).

[2] E. H. Hwang and S. Das Sarma, Dielectric function, screening, and plasmons in two-dimensional graphene, Phys. Rev. B **75**, 205418 (2007).

[3] M. Jablan, H. Buljan, and M. Soljacic, Plasmonics in graphene at infrared frequencies, Phys. Rev. B **80**, 245435 (2009).

[4] F. H. L. Koppens, D. E. Chang, and F. J. Garcia de Abajo, Graphene plasmonics: A platform for strong light-matter interactions, Nano Lett. **11**, 3370 (2011).

[5] P. A. D. Goncalves and N. M. R. Peres, *An Introduction to Graphene Plasmonics* (Word Scientific, Singapore, 2016).

[6] D. N. Basov, M. M. Fogler, and F. J. Garcia de Abajo, Polaritons in van der Waals materials, Science **354**, aag1992 (2016).

[7] J. Chen, M. Badioli, P. Alonso-Gonzalez, S. Thongrattanasiri, F. Huth, J. Osmond, M. Spasenovic, A. Centeno, A. Pesquera, P. Godignon, A. Zurutuza, N. Camara, F. J. Garcia De Abajo, R. Hillenbrand, and F. H. L. Koppens, Optical nano-imaging of gate-tunable graphene plasmons, Nature (London) **487**, 77 (2012).

[8] Z. Fei, A. S. Rodin, G. O. Andreev, W. Bao, A. S. McLeod, M. Wagner, L. M. Zhang, Z. Zhao, M. Thiemens, G. Dominguez, M. M. Fogler, A. H. Castro Neto, C. N. Lau, F. Keilmann, and D. N. Basov, Gate-tuning of graphene plasmons revealed by infrared nano-imaging, Nature (London) **487**, 82 (2012).

[9] G. F. Giuliani and G. Vignale, *Quantum Theory of the Electron Liquid* (Cambridge University Press, Cambridge, UK, 2005).

[10] I. V. Kukushkin, J. H. Smet, S. A. Mikhailov, D. V. Kulakovskii, K. von Klitzing, and W. Wegscheider, Observation of Retardation Effects in the Spectrum of Two-Dimensional Plasmons, Phys. Rev. Lett. **90**, 156801 (2003).

[11] V. M. Muravev, P. A. Gusikhin, I. V. Andreev, and I. V. Kukushkin, Novel Relativistic Plasma Excitations in a Gated Two-Dimensional Electron System, Phys. Rev. Lett. **114**, 106805 (2015).

[12] P. A. Gusikhin, V. M. Muravev, A. A. Zagitova, and I. V. Kukushkin, Drastic Reduction of Plasmon Damping in Two-Dimensional Electron Disks, Phys. Rev. Lett. **121**, 176804 (2018).

[13] V. I. Falko and D. E. Khmelnitskii, What if the film conductivity is higher than the speed of light?, Zh. Eksp. Teor. Fiz. **95**, 1988 (1989) [Sov. Phys. JETP **68**, 1150 (1989)].

[14] Resistance value in Eq. (1) can be estimated by combining the fine structure constant $\alpha = e^2/\hbar c \approx 1/137$ and the von Klitzing resistance quantum $h/e^2 = 25.8\text{k}\Omega$. The quantity $2\pi/c$ then translates into resistance of $2\pi(e^2/\hbar c)(\hbar/e^2) \approx 188\Omega$ per square.

[15] V. A. Volkov and V. N. Pavlov, Radiative plasmon polaritons in multilayer structures with a two-dimensional electron gas, JETP Lett. **99**, 93 (2014).

[16] H. Barlow and A. Cullen, Surface waves, Proc. IEEE - Pt. III: Radio Commun. Eng. **100**, 329 (1953).

[17] K. A. Michalski and J. R. Mosig, The Sommerfeld halfspace problem redux: Alternative field representations, role of Zenneck and surface plasmon waves, IEEE Trans. Ant. Prop. **63**, 5777 (2015).

[18] S. K. Oruganti, F. Liu, D. Paul, J. Liu, J. Malik, K. Feng, H. Kim, Y. Liang, T. Thundat, and F. Bien, Experimental realization of Zenneck type wave-based non-radiative, non-coupled wireless power transmission, Sci. Rep. **10**, 925 (2020).

[19] V. E. Babicheva, S. Gamage, L. Zhen, S. B. Cronin, V. S. Yakovlev, and Y. Abate, Near-field surface waves in few-layer MoS_2, ACS Photon. **5**, 2106 (2018).

[20] Z. M. A. El-Fattah, V. Mkhitaryan, J. Brede, L. Fernández, C. Li, Q. Guo, A. Ghosh, A. Rodríguez Echarri, D. Naveh, F. Xia, J. E. Ortega, and F. J. García de Abajo, Plasmonics in atomically thin crystalline silver films, ACS Nano **13**, 7771 (2019).